Memoirs of the Faculty of Engineering, Nagoya University
Vol. 27 No. 1 (1975) — Research Report —

ON SOME NUMERICAL SOLUTIONS OF THE FLOW THROUGH A BACK-STEP CHANNEL

SHIGEO UCHIDA and MAMORU ENDO

Department of Aeronautical Engineering

(Received May 27, 1975)

Abstract

Viscous flows of an incompressible fluid through a back-step channel, i. e., a channel with abrupt expansion of width, is investigated with special attention to the behavior of separated flow. Numerical solutions of Navier-Stokes equation is obtained by using the successive-over-relaxation method. Values of stream function and of vorticity are calculated for Reynolds number $Re=0$, 0.1, 1, 3, 10, 20, 30 and 40. Pressure distributions along the lower wall are obtained for some cases. It is found that, as described in some previous papers, the flow does not separate at the sharp edge of the corner. In the present paper the positions of separation point and of reattachment point are given as the function of Reynolds number.

1. Introduction

The separation of flow has been extensively investigated by many authors so far. However, we have not sufficient knowledge on the phenomena, since the mechanism of separation is so much complicated. Flows with sharp corner are mainly investigated by numerical integrations of Navier-Stokes equation, which have been done by Kawaguti[1)2)] for elbow and step channels, Macagno and Hung[3)] for an abruptly expanded tube and Roache and Mueller[4)] for a backward step.

In the present paper some numerical solutions for the fundamental configuration of back-step channel are computed to give some insight into the behavior of flow at the sharp corner and the situation of flow at separation point. The two-dimensional viscous flow of an incompressible fluid through a channel with a back step on one wall is considered as shown in Fig. 1. Successive-over-relaxation method, which is one of the finite difference methods, is adopted as a numerical procedure. It is shown that, in such flows, the separation point deviates from the sharp corner to the side of the back step.

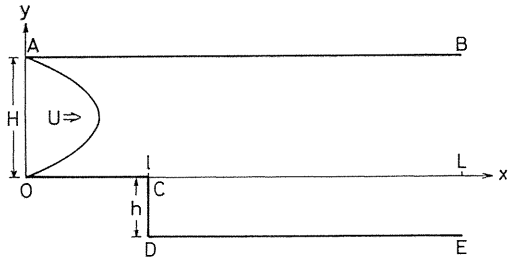

Fig. 1. The schematic model of a back-step channel.

2. Fundamental equations and boundary conditions

The co-ordinates system and dimensions of this model are defined in Fig. 1. It is assumed that the inflow into the entrance section OA is Poiseulle flow. The continuity and Navier-Stokes equations are made dimensionless with the reference quantities of the mean velocity U and the width H in the entrance section as follows:

$$\frac{\partial u}{\partial x}+\frac{\partial v}{\partial y}=0, \tag{1}$$

$$u\frac{\partial u}{\partial x}+v\frac{\partial u}{\partial y}=-\frac{\partial p}{\partial x}+\frac{1}{R_e}\left(\frac{\partial^2 u}{\partial x^2}+\frac{\partial^2 u}{\partial y^2}\right), \tag{2}$$

$$u\frac{\partial v}{\partial x}+v\frac{\partial v}{\partial y}=-\frac{\partial p}{\partial y}+\frac{1}{R_e}\left(\frac{\partial^2 v}{\partial x^2}+\frac{\partial^2 v}{\partial y^2}\right), \tag{3}$$

where pressure terms refer to ρU^2. Reynolds number is given by $Re=UH/\nu$, where ν is the kinematic viscosity. The stream function Ψ and the vorticity ζ are defined by

$$u=\frac{\partial \Psi}{\partial y}, \quad v=-\frac{\partial \Psi}{\partial x} \tag{4}$$

and

$$\zeta=\frac{\partial v}{\partial x}-\frac{\partial u}{\partial y}. \tag{5}$$

Substituting these quantities into Eqs. (1), (2) and (3), we have the fundamental equations for Ψ and ζ as follows:

$$\frac{\partial \Psi}{\partial y}\frac{\partial \zeta}{\partial x}-\frac{\partial \Psi}{\partial x}\frac{\partial \zeta}{\partial y}+\frac{1}{R_e}\left(\frac{\partial^2 \zeta}{\partial x^2}+\frac{\partial^2 \zeta}{\partial y^2}\right)=0, \tag{6}$$

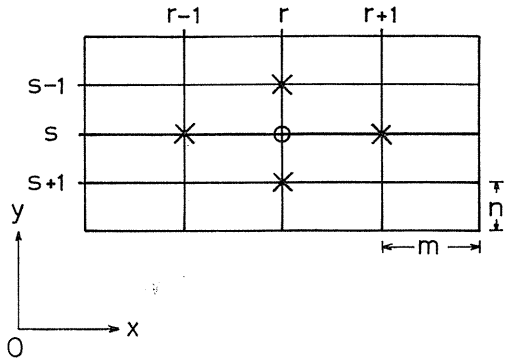

Fig. 2. Rectangular mesh geometry ($m=0.1$, $n=0.05$).

$$\frac{\partial^2 \Psi}{\partial x^2}+\frac{\partial^2 \Psi}{\partial y^2}=-\zeta. \tag{7}$$

If no-slip condition is considered on the walls, the boundary conditions are

$$\left.\begin{aligned} &\Psi=0,\ \partial\Psi/\partial \boldsymbol{n}=0 \quad \text{along } OCDE \\ \text{and}\quad &\Psi=1,\ \partial\Psi/\partial \boldsymbol{n}=0 \quad \text{along } AB \end{aligned}\right\} \tag{8}$$

The notation $\boldsymbol{n}$ denotes the direction normal to the wall. As the flow at the entrance section is Poiseulle flow, $u=6(y-y^2)$ from the assumption, the boundary conditions of Ψ and ζ at the entrance section are given by

$$\Psi=y^2(3-2y) \tag{9}$$

and

$$\zeta=6(2y-1). \tag{10}$$

The base pressure p_w along the lower wall is evaluated from Eqs. (2) and (3) with taking account of the boundary conditions.

$$\left.\begin{aligned} &\frac{\partial p_w}{\partial x}=\frac{1}{R_e}\left(\frac{\partial^2 u}{\partial y^2}\right)_w=-\frac{1}{R_e}\left(\frac{\partial \zeta}{\partial y}\right)_w \quad \text{along } OC,\ DE \\ &\frac{\partial p_w}{\partial y}=\frac{1}{R_e}\left(\frac{\partial^2 v}{\partial x^2}\right)_w=\frac{1}{R_e}\left(\frac{\partial \zeta}{\partial x}\right)_w \quad \text{along } CD \end{aligned}\right\} \tag{11}$$

Since the absolute value is arbitrary, the pressure distribution is calculated under the assumption that the base pressure is taken to be unity at point O.

3. Procedure of numerical computation

Dividing the flow region into small rectangular subregions as shown in Fig. 2, differentiations of the functions can be substituted by the finite difference between

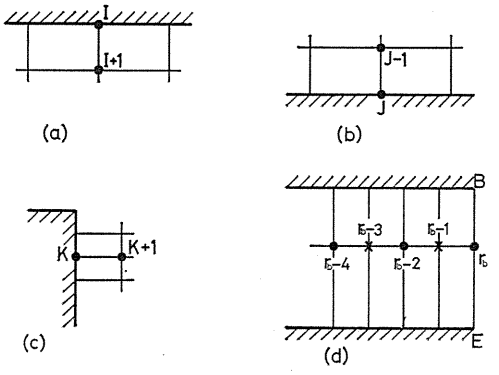

Fig. 3. Various types of the boundaries.
(a) The upper wall.
(b) The lower wall.
(c) The step wall.
(d) Outflow condition.

the concerning central point (r, s) and its four adjoining points for a sufficiently smooth region of flow. In order to apply the successive-over-relaxation method, Eqs. (6) and (7) are transformed to the form of finite difference equations as follows:

$$\Psi_{r,s}^{(k+1)}=\Psi_{r,s}^{(k)}+\omega\Big[\frac{n^2}{2(m^2+n^2)}(\Psi_{r+1,s}^{(k)}+\Psi_{r-1,s}^{(k+1)})+$$

$$\frac{m^2}{2(m^2+n^2)}(\Psi_{r,s+1}^{(k)}+\Psi_{r,s-1}^{(k+1)})+\frac{m^2n^2}{2(m^2+n^2)}\zeta_{r,s}^{(k+1)}-\Psi_{r,s}^{(k)}\Big], \tag{12}$$

$$\zeta_{r,s}^{(k+1)}=\zeta_{r,s}^{(k)}+\omega\Big[\frac{n^2}{2(m^2+n^2)}(\zeta_{r+1,s}^{(k)}+\zeta_{r-1,s}^{(k+1)})+\frac{m^2}{2(m^2+n^2)}(\zeta_{r,s+1}^{(k)}+\zeta_{r,s-1}^{(k+1)})$$

$$+\frac{mnR_e}{8(m^2+n^2)}\{(\Psi_{r+1,s}^{(k)}-\Psi_{r-1,s}^{(k+1)})(\zeta_{r,s-1}^{(k+1)}-\zeta_{r,s+1}^{(k)})$$

$$-(\Psi_{r,s-1}^{(k+1)}-\Psi_{r,s+1}^{(k)})(\zeta_{r+1,s}^{(k)}-\zeta_{r-1,s}^{(k+1)})\}-\zeta_{r,s}^{(k)}\Big], \tag{13}$$

where k is the iteration number and ω is the acceleration parameter for the convergence of numerical procedure, which is taken $0<\omega<2$.

The vorticity on the wall is expressed by Taylor expansion of the stream function and by the boundary conditions.

$$\zeta_I=3(1-\Psi_{I+1})/n^2-(1/2)\zeta_{I+1} \quad \text{on the upper wall.} \tag{14}$$

$$\zeta_J=-3\Psi_{J-1}/n^2-(1/2)\zeta_{J-1} \quad \text{on the lower wall.} \tag{15}$$

$$\zeta_K=-3\Psi_{K+1}/m^2-(1/2)\zeta_{K+1} \quad \text{on the step wall.} \tag{16}$$

The situation of ζ_I, ζ_J and ζ_K are shown in Fig. 3-a, 3-b and 3-c, respectively. The vorticity at the sharp corner C is evaluated by Eq. (15). Other schemes of this evaluation are examined in detail by Roache[5].

To calculate Ψ_{r_b} at the downstream section (see Fig. 3-d), it is expanded around point (r_b-2) as follows:

$$\Psi_{r_b}=\Psi_{r_b-2}+\left(\frac{\partial\Psi}{\partial x}\right)_{r_b-2}\cdot 2m+\frac{1}{2!}\left(\frac{\partial^2\Psi}{\partial x^2}\right)_{r_b-1}(2m)^2. \tag{17}$$

Since Ψ_{r_b-4} is also expanded in the form;

$$\Psi_{r_b-4}=\Psi_{r_b-2}-\left(\frac{\partial\Psi}{\partial x}\right)_{r_b-2}\cdot 2m+\frac{1}{2!}\left(\frac{\partial^2\Psi}{\partial x^2}\right)_{r_b-2}(2m)^2, \tag{18}$$

the first and the third terms of right hand in Eqs. (17) and (18) can be eliminated, which giving

$$\Psi_{r_b}=\Psi_{r_b-4}+4m\left(\frac{\partial\Psi}{\partial x}\right)_{r_b-1}.$$

By the use of central difference for $(\partial\Psi/\partial x)_{r_b-2}$ the value of Ψr_b can be expressed by

$$\Psi_{r_b}=\Psi_{r_b-4}+2(\Psi_{r_b-1}-\Psi_{r_b-3}). \tag{19}$$

The similar treatment is applied to the boundary value for ζ, too.

Boundary values of Ψ and ζ are finally expressed by

$$\Psi^{(k+1)}_{r_b,s}=\Psi^{(k+1)}_{r_b-4,s}-2\Psi^{(k+1)}_{r_b-3,s}+2\Psi^{(k+1)}_{r_b-1,s} \quad \text{on } BE, \tag{20}$$

$$\zeta^{(k+1)}_{r_b,s}=\zeta^{(k+1)}_{r_b-4,s}-2\zeta^{(k+1)}_{r_b-3,s}+2\zeta^{(k+1)}_{r_b-1,s} \quad \text{on } BE. \tag{21}$$

The initial values in iteration are taken from the values of Poiseulle flow.

In the course of computation the stream function and the vorticity are regarded to be converged, when the totals of absolute values of E_1 (r, s) and $E_2(r, s)$ in all inner points, i.e.,

$$NORM_1=\sum|E_1(r, s)| \quad \text{and} \quad NORM_2=\sum|E_2(r, s)|$$

become less than 0.5×10^{-2}, where E_1 (r, s) and E_2 (r, s) are written in terms of the brackets in the right hand of Eqs. (12) and (13), respectively.

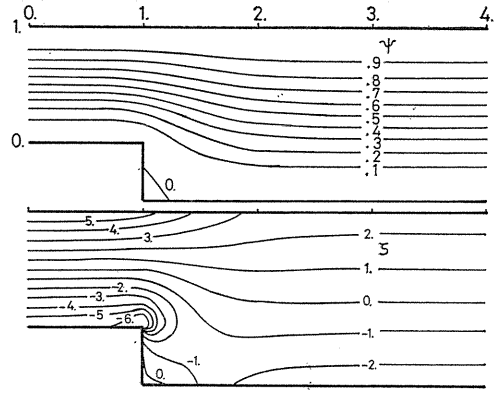

Fig. 4. Stream function and vorticity ($Re=0$).

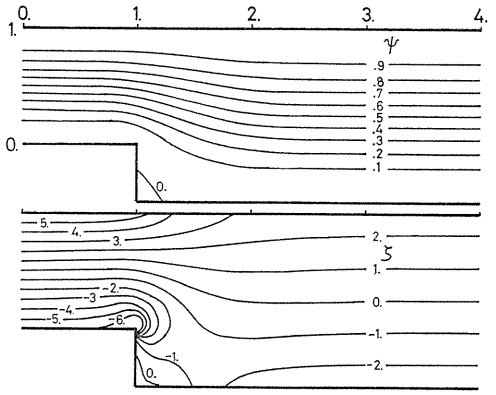

Fig. 5. Stream function and vorticity ($Re=0.1$).

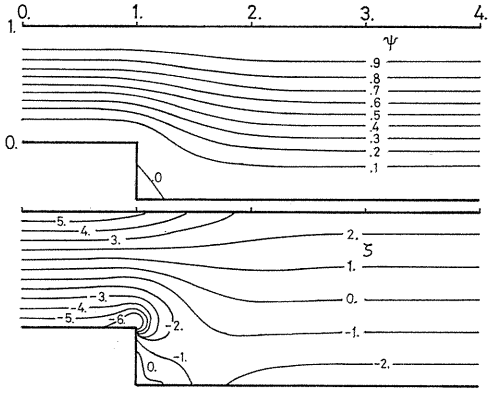

Fig. 6. Stream function and vorticity ($Re=1$).

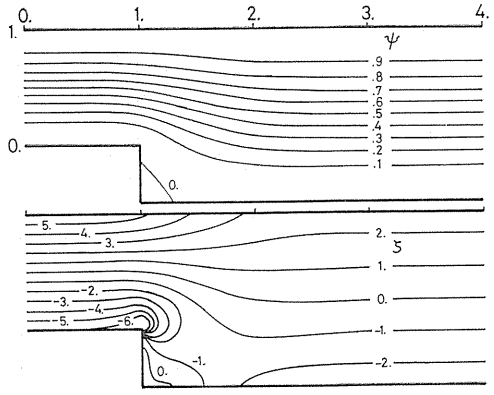

Fig. 7. Stream function and vorticity (Re=3).

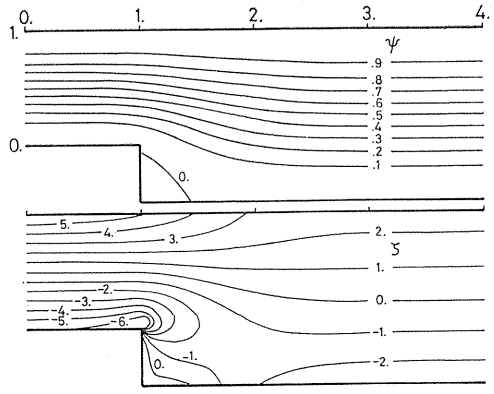

Fig. 8. Stream function and vorticity (Re=10).

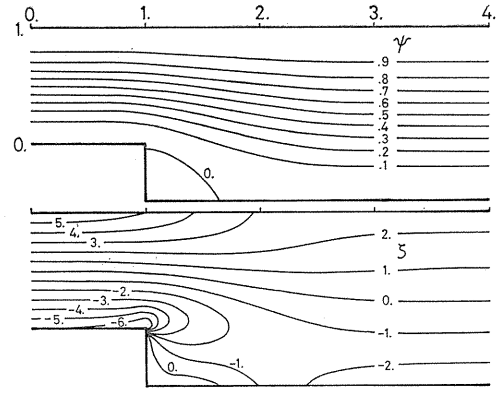

Fig. 9. Stream function and vorticity (Re=20).

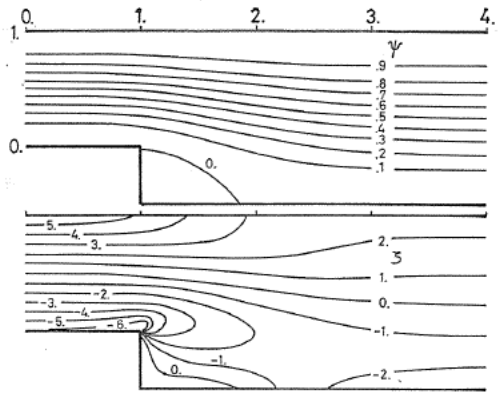

Fig. 10. Stream function and vorticity (Re=30).

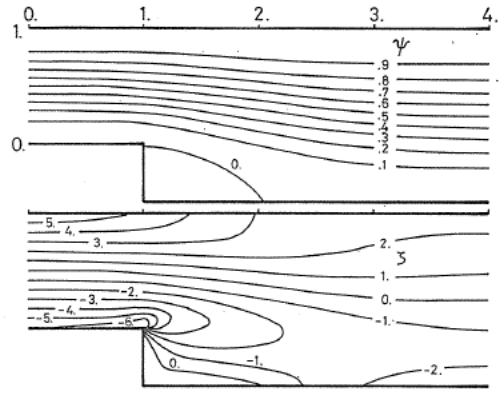

Fig. 11. Stream function and vorticity (Re=40).

4. Numerical results and discussions

Choosing a back-step channel of L/H=4.5, l/H=1.0, h/H=0.5, m=0.1 and n=0.05 as shown in Figs. 1 and 2, the numerical solutions for Reynolds number Re= 0, 0.1, 1, 3, 10, 20, 30 and 40 are obtained. In this computation, the acceleration parameter ω is taken to be unity.

Even for the lowest limit of Stokes flow, Re=0, it is found that the flow separates from the corner as shown in Fig. 4. The recirculating region grows large according to increase of Reynolds number (see Figs. 4 to 11). The distance h_r from the concave corner D to the reattachment point increases linearly in proportion to Reynolds number as shown in Fig. 12. Denoting the distance from D to the separation point by h_s, h_s/h is found to be 0.56 for Re=0 and approaches rapidly to unity for Re>1 as shown in Fig. 13. The distributions of base pressure is shown in Fig. 14 refering to the stepped co-ordinate along $OCDE$. The base pressure p_w drops at the convex corner and keeps on decreasing even after separation. Sub-

sequently, it rises and reaches to a peak value behind the reattachment point. Then, it approaches to the constant pressure gradient in the far downstream.

It is found that the separation point moves toward the concave corner in decreasing Reynolds number, which is the same tendency as in the flow past a circular cylinder. In the latter case, however, the flow does not separate in the low Reynolds number region near $Re=0$, namely in the non-vortex region[6]. This means that if the boundary has a sharp corner, separation occurs even in the very slow flow. Recently, Matsui and Hiramatsu investigate that the displacement of the separation point occurs in the low speed flow around a sharp corner[7].

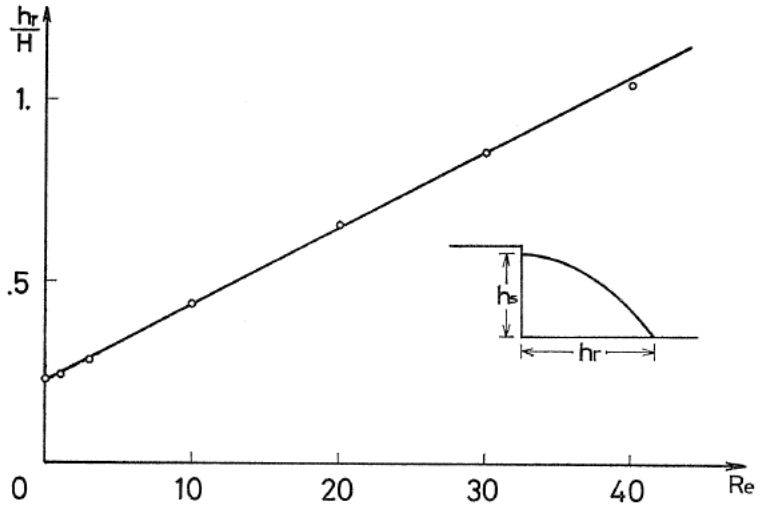

Fig. 12. Location of reattachment point.

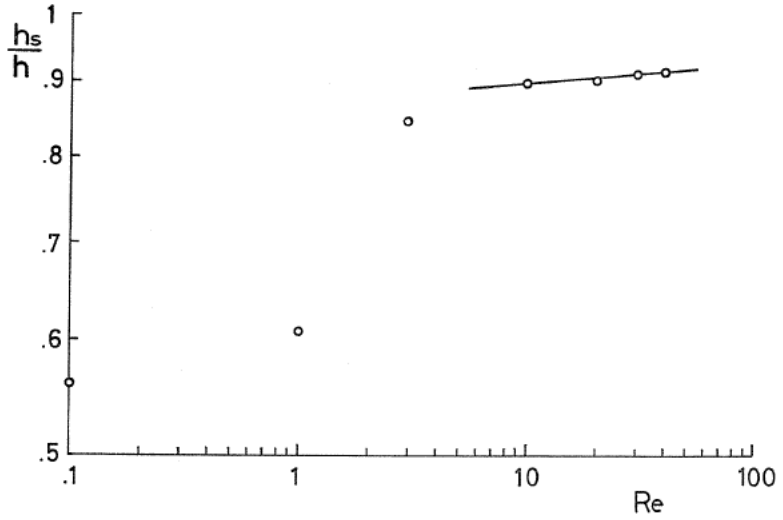

Fig. 13. Location of separation point.

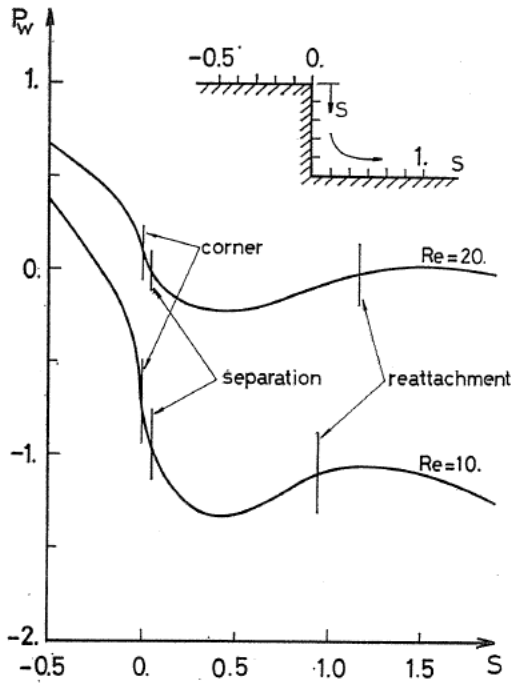

Fig. 14. Distributions of base pressure (R_e=10, 20).

References

1) Kawaguti, M.: Numerical Solutions of the Navier-Stokes Equations for Flow in a Channel with a Step, MRC Technical Summary Report 574, University of Wisconsin, May 1965.
2) Kawaguti, M.: Numerical Study of the Flw of a Viscous Fluid in a Curved Channel, Phys. Fluids, suppl., pp. 101—104, 1969.
3) Macagno, E. O. and Hung, T. K.: Computational and Experimental Study of a Captive Annular Eddy, J. Fluid Mech., vol. 28, pp. 43—64, 1967.
4) Roache, P. J. and Mueller, T. J.: Numerical Solutions of Laminar Separated Flows, AIAA J., vol. 8, pp. 530—538, 1970.
5) Roache, P. J.: Computational Fluid Dynamics, Hermosa Publishers, Albuquerque, 1972.
6) Matsui, T.: Separation in a Flow past a Circular cylinder, J. Japan Soc. Aero. Space Sci., vol. 20, pp. 610—618, 1972. (in Japanese).
7) Matsui, T. and Hiramatsu, M.: Separation of Low Reynolds Number Flow around a Corner, 2nd Symposium on Flow Visualization, pp. 131—134, ISAS, Univ. of Tokyo, 1974. (in Japanese).